

RESEARCH ARTICLE

Δ 9-Tetrahydrocannabinol inhibits Hedgehog-dependent patterning during development

Hsiao-Fan Lo¹, Mingi Hong¹, Henrietta Szutorisz², Yasmin L. Hurd² and Robert S. Krauss^{1,*}

ABSTRACT

Many developmental disorders are thought to arise from an interaction between genetic and environmental risk factors. The Hedgehog (HH) signaling pathway regulates myriad developmental processes, and pathway inhibition is associated with birth defects, including holoprosencephaly (HPE). Cannabinoids are HH pathway inhibitors, but little is known of their effects on HH-dependent processes in mammalian embryos, and their mechanism of action is unclear. We report that the psychoactive cannabinoid Δ 9-tetrahydrocannabinol (THC) induces two hallmark HH loss-of-function phenotypes (HPE and ventral neural tube patterning defects) in *Cdon* mutant mice, which have a subthreshold deficit in HH signaling. THC therefore acts as a 'conditional teratogen', dependent on a complementary but insufficient genetic insult. *In vitro* findings indicate that THC is a direct inhibitor of the essential HH signal transducer smoothed. The canonical THC receptor, cannabinoid receptor-type 1, is not required for THC to inhibit HH signaling. Cannabis consumption during pregnancy may contribute to a combination of risk factors underlying specific developmental disorders. These findings therefore have significant public health relevance.

KEY WORDS: THC, Cannabis, Hedgehog, Holoprosencephaly, Birth defect, CDON, Mouse

INTRODUCTION

Congenital malformations affect approximately 8 million newborns worldwide each year and are a leading cause of death for infants and children of all ages (Christianson et al., 2006; Krauss and Hong, 2016; Wallingford, 2019). In some cases, mutations in single genes or exposure to individual teratogens is sufficient to cause a developmental disorder in most or all those affected (Amberger et al., 2019; Gilbert-Barnes, 2010; Webber et al., 2015). For many of the most common structural birth defects, however, a single causative factor cannot be identified, and the underlying etiology for such disorders is poorly understood. In these cases, it is likely that genetic and environmental risk factors interact to elevate the chance of a defect occurring in specific developmental processes (Beames and Lipinski, 2020; Fraser, 1980; Krauss and Hong, 2016; Lovely et al., 2017). Genome sequencing has led to identification of numerous birth defect-associated variants, many of which appear to

predispose individuals to a given anomaly and presumably act with additional factors (Webber et al., 2015). Identification of subthreshold environmental risk factors by epidemiology is more difficult.

Cannabis is the illicit drug most commonly used during pregnancy and, with expanded legalization and decreased perception of risk, use is increasing (Volkow et al., 2017; Young-Wolff et al., 2017). Meta-analysis of studies through 2014 concluded that maternal cannabis use is associated with low birth weight and increased likelihood of requirement for neonatal intensive care (Gunn et al., 2016). Recently, in Colorado, a correlation was reported between: (1) increased cannabis usage during pregnancy; (2) increased fetal phytocannabinoid exposure levels; and (3) an increase in major structural developmental defects (Reece and Hulse, 2019). Use of other drugs and tobacco remained static or fell in Colorado during the reporting period. A similar pattern was observed with rising incidence of atrial septal defects in multiple US states and Australia (Reece and Hulse, 2020). These correlations suggest that cannabinoids might be teratogenic, but they do not demonstrate causality.

A common birth defect that serves as a model for gene-environment interactions and multifactorial etiology is holoprosencephaly (HPE) (Beames and Lipinski, 2020; Hong and Krauss, 2018; Roessler et al., 2018). HPE is caused by failure to define the midline of the forebrain and/or midface. HPE comprises a phenotypic continuum ranging from complete failure to partition the forebrain into hemispheres with accompanying cyclopia, through to mild midfacial midline deficiency (Cohen, 2006; Muenke and Beachy, 2001). The Hedgehog (HH) signaling pathway is a key regulator of many developmental processes, including patterning of the forebrain and facial midline, limbs and digits, and ventral neural tube (VNT) (Petryk et al., 2015; Sagner and Briscoe, 2019; Tickle and Towers, 2017). HPE is associated with heterozygous mutations in the HH pathway (Dubourg et al., 2018; Roessler et al., 2018). Clinical presentation of HPE is highly variable, and many mutation carriers are unaffected, even in pedigrees. These observations have led to a multifactorial, 'mutation plus modifier' model, in which heterozygous mutations may be insufficient for severe phenotypes and their penetrance and expressivity are graded by additional genetic variants and/or environmental exposures (Dubourg et al., 2018; Hong and Krauss, 2018; Roessler et al., 2012).

HH ligands activate a conserved signaling pathway (Kong et al., 2019; Lee et al., 2016; Petrov et al., 2017). In the absence of HH, the primary receptor patched 1 (PTCH1) acts to inhibit the activity of a second membrane protein, smoothed (SMO). Binding of HH to PTCH1 relieves inhibition of SMO. SMO then signals to activate pathway target genes via GLI transcription factors. SMO is a class F, G protein-coupled receptor (GPCR). PTCH1 appears to function as a transporter to restrict accessibility of SMO to its activating ligands, namely cholesterol and oxysterols. HH ligands block PTCH1

¹Department of Cell, Developmental, and Regenerative Biology, New York, NY 10029, USA. ²Addiction Institute and Departments of Psychiatry and Neuroscience, Icahn School of Medicine at Mount Sinai, New York, NY 10029, USA.

*Author for correspondence (Robert.Krauss@mssm.edu)

 R.S.K., 0000-0002-7661-3335

Handling Editor: James Briscoe
Received 3 March 2021; Accepted 23 August 2021

function, allowing SMO access to cholesterol and oxysterols, thus activating SMO signaling (Qi and Li, 2020; Radhakrishnan et al., 2020). These events occur in the primary cilium, an organelle in which HH pathway components are trafficked and concentrated for signaling (Bangs and Anderson, 2017; Gigante and Caspari, 2020). Consistent with the notion that SMO is itself a ligand-regulated receptor, many small molecules that act as SMO agonists or antagonists have been identified (Sharpe et al., 2015). Although PTCH1 function is sufficient for SMO inhibition, HH signal reception also requires at least one of three co-receptors (CDON, BOC, GAS1). CDON, BOC and GAS1 have overlapping roles and are collectively required for HH signaling (Allen et al., 2011; Izzi et al., 2011; Wierbowski et al., 2020; Zhang et al., 2011). Mice with targeted mutations in any one of these co-receptors have a selective and partial loss of HH pathway function.

In a search for endogenous lipids that act as SMO antagonists, Eaton and colleagues identified endocannabinoids as inhibitors of HH signaling (Khaliullina et al., 2015). Endocannabinoids were effective as HH pathway inhibitors in both developing *Drosophila* wing disks and cultured mammalian cells. Endocannabinoids are fatty acids/alcohols linked to polar head groups that signal through the GPCRs cannabinoid receptor-type 1 (CB1R; CNR1) and -type 2 (CB2R; CNR2) (Lu and Mackie, 2020; Maccarrone et al., 2015). Phytocannabinoids are bioactive ingredients of cannabis and include Δ^9 -tetrahydrocannabinol (THC) and cannabidiol (CBD), the former being the major psychoactive component. These compounds exert their effects via CB1R, CB2R, and/or other receptors, with CB1R responsible for mediating the major neurobehavioral effects of THC (Lu and Mackie, 2020; Schurman et al., 2020). Importantly, THC and CBD inhibit HH signaling in a similar manner to endocannabinoids, whereas structurally unrelated CB1R and CB2R agonists/antagonists do not (Khaliullina et al., 2015). Cannabinoids have been proposed to inhibit HH signaling at the level of SMO, although this mechanism was not uniform among those analyzed and has been questioned by others (Sever et al., 2016).

These findings raise the possibility that *in utero* exposure to phytocannabinoids might be teratogenic, owing to an ability to inhibit HH signaling at crucial points during development. We report here that THC is teratogenic to genetically sensitized mice harboring a subthreshold deficit in HH pathway signaling strength. THC dose-dependently induced HH loss-of-function phenotypes, including HPE, in these mice but not in wild-type mice. THC therefore acted as a 'conditional teratogen', dependent on a complementary but insufficient genetic insult. Furthermore, in *in vitro* assays, THC displayed properties similar to the *bone fide* SMO inhibitor SANTI1. Together, these results raise the possibility that human cannabis consumption during early pregnancy may expose embryos to HH inhibition, presenting an environmental risk factor for birth defects.

RESULTS

THC-exposed *Cdon*^{-/-} embryos display HPE with craniofacial midline defects

Cdon^{-/-} mice on a 129S6 background have a subthreshold defect in HH signaling and are sensitive to induction of HPE by both genetic and environmental modifiers (Hong and Krauss, 2018). They therefore model human HPE and are an ideal model in which to assess THC teratogenicity. 129S6 *Cdon*^{+/-} mice were intercrossed and pregnant females received a single dose of THC at 5, 10 or 15 mg/kg, administered intraperitoneally at embryonic day (E) 7.5. The E7.5 time point was used because it was most effective for

induction of HPE in wild-type mice by the potent SMO inhibitor vismodegib (Heyne et al., 2015). We measured blood concentrations of THC and metabolites in pregnant female mice, and the peak levels achieved at the highest THC dose used were similar to those achieved by humans after inhalation of 34 mg cannabis (180-200 ng/ml) (Grotenhermen, 2003) (Fig. S1).

Embryos were harvested at E14 and scored as positive for HPE if they displayed a fused upper lip, an unambiguous phenotype without gradation that arises as a consequence of defective craniofacial midline patterning (Hong and Krauss, 2012). Vehicle- and THC-treated *Cdon*^{+/+} and *Cdon*^{+/-} embryos did not have HPE, nor did vehicle-treated *Cdon*^{-/-} embryos. In contrast, THC-exposed *Cdon*^{-/-} embryos displayed mid-facial HPE phenotypes in a dose-responsive manner (Fig. 1A,B; Table S1). Hematoxylin and Eosin (H&E)-stained sections revealed that THC-treated *Cdon*^{-/-} embryos had fully partitioned forebrains, but displayed substantial diminution of midfacial structures, including close-set and rudimentary vomeronasal organs, and reduced width of the nasal septum cartilage (Fig. 1A-A''; Fig. S2). These results classify THC-induced HPE in *Cdon*^{-/-} mice as the relatively mild, lobar category (Krauss, 2007). Whole-mount *in situ* hybridization at E10 revealed reduction in expression of two direct SHH target genes, *Gli1* and *Nkx2-1*, in the rostroventral midline of THC-treated *Cdon*^{-/-} embryos (Fig. 1C).

To investigate the effects of THC on gene expression more quantitatively, RNA was extracted from dissected forebrains of E9.0 embryos, and quantitative RT-PCR (qRT-PCR) was performed for several SHH target genes. Although there was some variability, possibly related to partial penetrance, mRNA levels of *Gli1*, *Nkx2-1* and *Shh* were significantly reduced in THC-treated *Cdon*^{-/-} embryos (Fig. 1D). *Ptch1* mRNA levels trended lower in THC-treated *Cdon*^{-/-} embryos, although this was not statistically significant owing to variability between the samples ($P=0.08$). In contrast, levels of *Bmp4* mRNA, which controls CNS patterning dorsally and medially and is not known to be directly regulated by HH signaling, was similar between controls and THC-treated *Cdon* mutants (Fig. 1D). Additionally, these results may underestimate the reduction in expression of SHH target genes in the most affected region of THC-treated *Cdon*^{-/-} embryos because non-midline structures were by necessity present in the dissected tissue. Taken together, these results show that *Cdon* mutation and THC synergized to induce HPE in mice.

THC induces VNT patterning defects in *Cdon*^{-/-} mice

We next sought to assess the effects of *in utero* exposure to THC on a second HH-dependent patterning process. Sonic HH (SHH) produced by the notochord and floor plate (FP) forms a ventral-to-dorsal gradient of pathway activity in the developing neural tube. In response to distinct levels of SHH pathway activity, expression of specific transcription factors is induced in specific progenitor zones of the VNT. These proteins include: FOXA2 (in the FP), NKX2-2 (in p3 progenitors) and OLIG2 (in pMN motor neuron progenitors). Pregnant dams were treated with a single dose of THC (15 mg/kg) at E8.0 and embryos were analyzed at E9.5, by immunofluorescence (IF) analysis of forelimb-level sections. The E8.0 time point was used because it was effective for inhibition of SHH-dependent VNT patterning in wild-type embryos by the SMO inhibitor cyclopamine (Ribes et al., 2010). THC reduced the number of FOXA2⁺ FP cells by >50% and of NKX2-2⁺ p3 progenitors by >35% in *Cdon*^{-/-} embryos (Fig. 2). The more dorsally positioned OLIG2⁺ pMN progenitors, which require a lower level of HH signal to be induced, were not affected (Fig. 2). These results are very similar to those

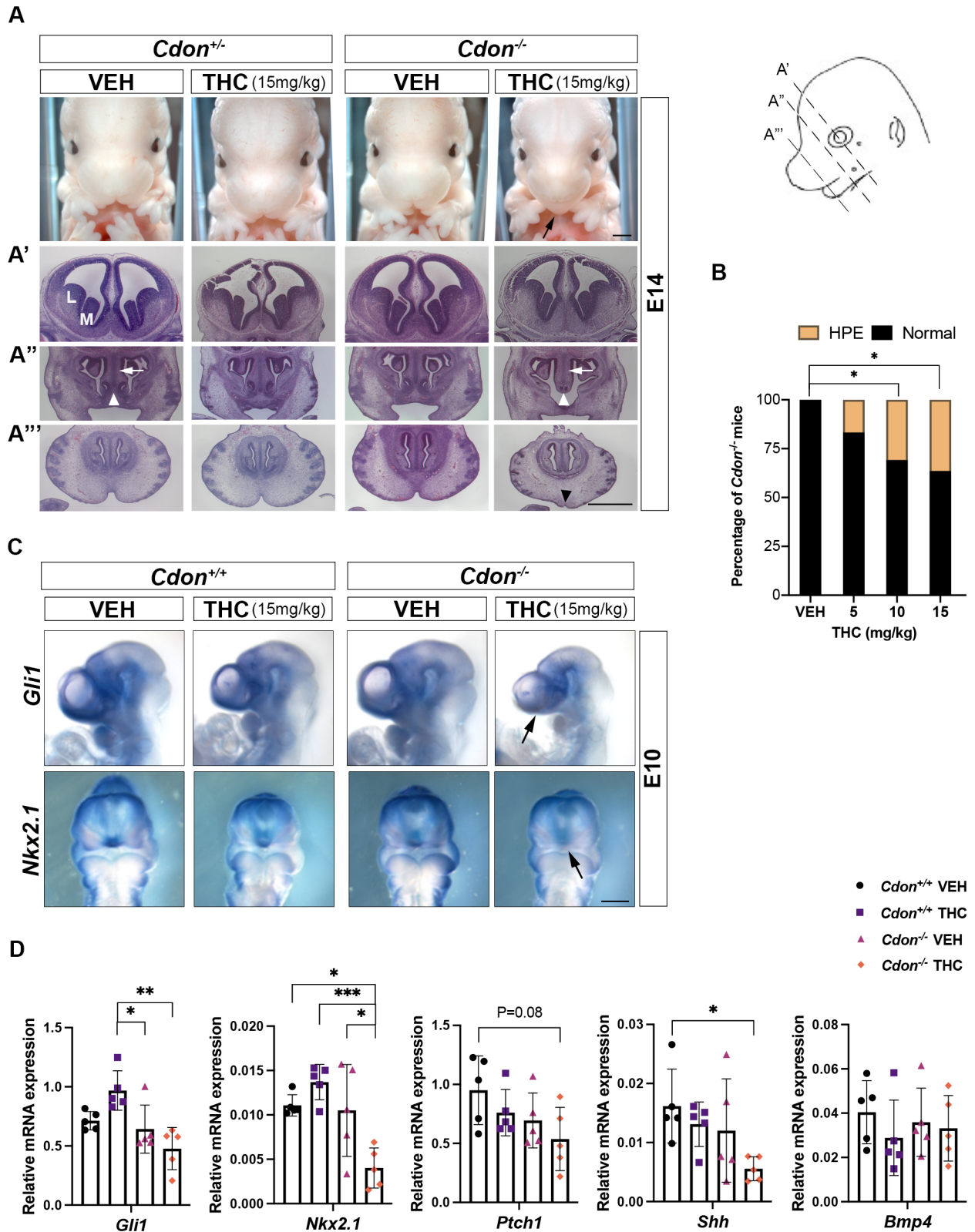


Fig. 1. See next page for legend.

obtained by removal of one copy of *Shh* from *Cdon*^{-/-} mice (Tenzen et al., 2006). Taken together, our findings demonstrate that THC is teratogenic in genetically sensitized mice, producing two well-established, SHH loss-of-function phenotypes: HPE and defective VNT patterning.

THC is likely a direct inhibitor of SMO

Khaliullina et al. reported that THC inhibited a HH-dependent reporter construct in NIH3T3 cells, a well-established cell culture system for studying HH signaling and the mechanisms of pathway inhibitors (Khaliullina et al., 2015; Taipale et al., 2000). We

Fig. 1. THC induces HPE in *Cdon*^{-/-} mutant mice. (A-A'') Frontal views of forebrains and faces of embryos with indicated genotypes and treatments. HPE phenotypes in THC-treated *Cdon*^{-/-} mice include fusion of the upper lip (black arrow), close-set and rudimentary vomeronasal organs (white arrowheads), reduced nasal septal cartilage (white arrows) and loss of midfacial midline structure (black arrowhead). Mice were administered THC or vehicle (VEH) at E7.5 and harvested at E14. Top row: whole-mount E14 embryos. Next three rows: H&E-stained sections of E14 embryos. L, lateral ganglionic eminence; M, medial ganglionic eminence. The angle and level of H&E sections are displayed in the diagram on the right, as A', A'' and A'''. (B) THC induces HPE in *Cdon*^{-/-} mice in a dose-dependent manner. The numbers of embryos scored as positive for HPE were 2/12, 4/13 and 4/11 at 5 mg/kg, 10 mg/kg and 15 mg/kg THC, respectively; also see Table 1. **P*<0.05 (two-tailed Fischer's exact test). (C) Whole-mount *in situ* hybridization of E10 embryos exposed *in utero* to THC (15 mg/kg) or VEH. Expression of two direct SHH target genes (*Gli1* and *Nkx2-1*) is reduced in the rostroventral midline (arrows). Embryos had 30-35 pairs of somites. (D) Inhibition of SHH target gene expression by THC. Pregnant females were administered 15 mg/kg THC or VEH at E8.0 and embryos of the indicated genotypes assessed. Embryo forebrains were isolated at E9.0 (17-20 pairs of somites) for qRT-PCR analysis of *Gli1*, *Nkx2-1*, *Ptch1*, *Shh* and *Bmp4* expression, all normalized to *Gapdh* expression. Values are mean±s.d. from five individual embryos **P*<0.05, ***P*<0.01, ****P*<0.001 (ordinary one-way ANOVA). Scale bars: 1 mm.

confirmed this observation. Treatment of NIH3T3 cells with recombinant SHH induced an ~10-fold increase in expression of the direct, endogenous target gene *Gli1* as measured by qRT-PCR (Fig. 3A). THC dose-dependently inhibited *Gli1* induction in response to SHH, with an IC₅₀ of ~1 μM. Similar results were obtained when these cells were stimulated with the direct SMO agonist SAG (Fig. S3A), and with SHH treatment of a second cell system, freshly prepared mouse embryo fibroblasts (MEFs) (Fig. S3B).

It has been reported that cannabinoids inhibit HH signaling at the level of SMO, although differences were seen between the cannabinoids examined, and THC was not tested (Khaliullina et al., 2015). PTCH1 and SUFU are negative regulators of HH signaling. MEFs that are null for either gene display constitutive pathway activity, with PTCH1 functioning upstream of SMO, and SUFU acting downstream of SMO (Kong et al., 2019; Lee et al., 2016; Petrov et al., 2017). To identify the position within the HH pathway at which THC acts, we first tested its ability to inhibit constitutive expression of *Gli1* in *Ptch1*^{-/-} and *Sufu*^{-/-} MEFs. THC attenuated *Gli1* expression in *Ptch1*^{-/-} MEFs, but not in *Sufu*^{-/-} MEFs, in a dose-dependent manner (Fig. 3B). Therefore, THC modulates SHH signaling downstream of PTCH1 and upstream of SUFU. Although these data place the likely point of action of THC at the level of SMO, this could occur via direct SMO inhibition or indirectly, e.g. via perturbation of primary cilia, the cellular site of signaling to GLI.

SMO activation is a two-step process. Ciliary transport of SMO (step 1) is followed by SMO activation within cilia (step 2) (Fig. 3C) (Rohatgi et al., 2009; Wilson et al., 2009). A low level of SMO trafficks through primary cilia constitutively. Some direct SMO inhibitors, such as SANT1, induce a SMO conformation that inhibits trafficking and prevents ciliary accumulation in response to activators, such as SHH and SAG. Another class of SMO inhibitor, exemplified by cyclopamine, induces a SMO conformation that does not inhibit trafficking, but which resists activation within cilia. Therefore, cyclopamine-type inhibitors trap SMO in primary cilia even in the absence of SHH or SAG, yet block activation of SMO within cilia, even in the presence of these pathway activators (Rohatgi et al., 2009; Wilson et al., 2009). We assessed the effect of THC on ciliary translocation of endogenous SMO in NIH3T3 cells treated with various HH pathway-regulating compounds (Fig. 3D,E; Table 1). The percentage of cells with ciliary SMO and fluorescence

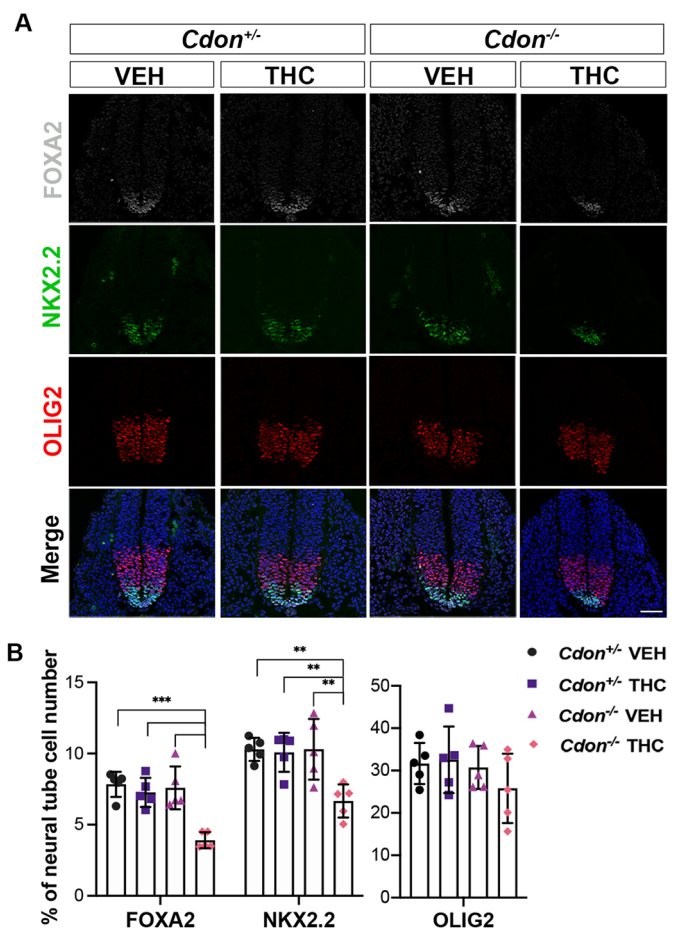


Fig. 2. THC induces VNT patterning defects. (A) Immunofluorescence analysis of forelimb level sections of embryos with indicated genotypes. Pregnant females were administered 15 mg/kg THC or VEH at E8.0 and analyzed at E9.5 (20-24 pairs of somites). All nuclei are visible by DAPI stain (blue) in the merged images. Scale bar: 50 μm. (B) Numbers of FOXA2⁺, NKX2-2⁺ and OLIG2⁺ cells relative to whole neural tube cells were quantified. Values are means from three to five sections from five individual mice. ****P*<0.05, ***P*<0.01, ****P*<0.001 (ordinary one-way ANOVA with Tukey's multiple comparison test). See Table S2 for numbers of FOXA2⁺, NKX2-2⁺, OLIG2⁺ and total cells in neural tubes of individual embryos.

intensity of ciliary protein expression were determined. THC alone did not trigger SMO translocation to cilia, but it blocked SMO accumulation in cilia in response to SHH, cyclopamine or SAG. THC also inhibited constitutive ciliary localization of SMO in *Ptch1*^{-/-} MEFs. THC did not affect cilium length or ciliary levels of the primary cilia marker ARL13B (Fig. S4A,B). Therefore, THC acts similarly to SANT1, preventing SMO translocation into primary cilia.

The phytocannabinoid CBD is structurally related to THC and has also been reported to inhibit HH signaling (Khaliullina et al., 2015). In contrast to our results with THC, Khaliullina et al. found that CBD did not prevent localization of exogenously expressed SMO to primary cilia in response to SAG (Khaliullina et al., 2015). Because these results and our own findings with THC were dichotomous, we tested CBD as well. CBD inhibited SHH-induced *Gli1* expression in NIH3T3 cells with an IC₅₀ of ~1.2 μM, a value similar to that of THC (Fig. 4A). Like THC, CBD alone did not promote translocation of SMO to primary cilia (Fig. 4B,C). We found that CBD did reduce endogenous SMO ciliary translocation in response to SHH. However, despite having similar IC₅₀ values,